iJRASET
International Journal For Research in Applied Science and Engineering Technology

INTERNATIONAL JOURNAL FOR RESEARCH

IN APPLIED SCIENCE & ENGINEERING TECHNOLOGY

Volume: 8 **Issue:** III **Month of publication:** March 2020

DOI:

www.ijraset.com

Call: 08813907089 | E-mail ID: ijraset@gmail.com

International Journal for Research in Applied Science & Engineering Technology (IJRASET)
ISSN: 2321-9653; IC Value: 45.98; SJ Impact Factor: 7.429
Volume 8 Issue III Mar 2020- Available at www.ijraset.com

Electrical and Structural Characterization of Fired SnO_2 Thick Films by Screen Printing Technique

R. M. Nikam[1], K. H. Kapadnis[2], R. Y. Borse[3]
[1]*Department of Chemistry, M. J. M. ACS College, Karanjali, Tal- Peth, Dist-Nashik-422 208,*
[2]*Department of Chemistry, L. V. H. ACS College, Panchavati, Dist-Nashik-422 003,*
[3]*Department of Physics, M. J. M. ACS College, Karanjali, Tal- Peth, Dist-Nashik-422 208.*

Abstract: ***Thick films of SnO_2 were prepared by Standard Screen printing method on glass substrates and films are annealed at 450^0C in air atmosphere. Electrical characterization was studied in static system. This paper revealed that SnO_2 is n-type semiconductor obeying negative temperature coefficient (NTC) characteristics. Thick films of SnO_2 were characterized by SEM, EDAX, XRD, FTIR and UV to study surface morphology, elemental analysis, crystalline Phases of films, vibrational and optical modes respectively.***

Keywords: Thick Films, Screen printing method, XRD, SEM, EDAX.

I. INTRODUCTION

The air is a mixture of different pollutant gases. Nowadays in order to monitor these gases different techniques are used. Micro-sensors constructed with SnO_2 material is found to be more versatile because of its use in transistors, electrodes, gas sensors, liquid crystal displays, catalysts, photovoltaic devices, photo sensors, antistatic coatings, polishing and ceramic glazes [1]. Tin oxide is useful due to high degree of transparency in the visible spectrum, low operating temperature, strong thermal stability and more stable in higher oxidation state (+4) thereby a good oxidising agents in organic synthesis. Tin oxide is colourless, diamagnetic and amphoteric solid with n-type semiconductor having wide band gap 3.7 eV [2]. Krishnakumar. T. et. al., have reported that tin oxide exist as tetragonal (SnO_2) cassiterite oriented in most sharp XRD peak (110) in mineral form and rhomarchite (SnO) form oriented in most sharp XRD peak (101). Tin oxide semiconductor has space group $P4_2/mmm$ and unit cell parameters are a=4.737 Å, c=3.185 Å [3]. In crystal lattice of SnO_2, Sn^{4+} ions are six co-ordinated octahedrally surrounded with three co-ordinated trigonal planer O^{2-} ions.

II. LITERATURE SURVEY

Tin element 50 hides everywhere in our nature often in movie relics: from *The Wizard of Oz's* Tin Man to tin can radio often spotted in tree houses. It exist in crystalline β and brittle α form at low temperature, two other exist at high temperature and pressure [4]. Nanostructured material has been extensively applied in technological applications because of their novel characteristic electronic, optical and mechanical properties and unique shape [5]. Gas sensitive materials of metal oxide having porous structure of thick films have been extensively studied and implemented for their gas response to oxidising and reducing gases. Practical gas sensors are made up porous material such as SnO_2, ZnO, WO_3, In_2O_3 etc. Among all tin oxide (SnO_2) of tetragonal phase material is universally accepted gas sensor [6].

It provides a high surface volume ratio and exact mechanism of gas sensing based on adsorption-desorption phenomenon. Tin oxide blended with other metal oxide i.e. binary oxide solid mixtures are found be more versatile than doped with noble metal and single counterpart. Semiconductor based chemiresistors are mostly investigated known as chemiresistive gas sensors. These fabricated sensors have excellent sensitivity, very short response time and low cost [5-6].

III. EXPERIMENTAL

A. Preparation of SnO_2 Thick Films:

Tin-oxide thick films were prepared on glass substrate with particular dimension by using standard screen-printing technique [7-13]. The SnO_2 powder (99.99 %) of loba grade was weighed and dried in air at 450^0C for 5 hr. The calcined SnO_2 powder was mixed and crushed thoroughly with glass frit acts as permanent binder and ethyl cellulose acts as a temporary binder. The mixture was then mixed with butyl carbitol acetate as organic vehicle to form the paste. The paste was then screen printed onto the surface of glass substrate. The details of the technique are described elsewhere [9]. After screen printing the films were dried under IR- lamp for 1 hr. and then fired at 450^0C for 5 hrs. The thickness of the films was observed in the range of 20μm–30μm.

1) Electrical Measurement

The resistance of the thick film sample was measured by using half bridge method at different temperatures in air. Variable DC power supply (APLAB 0-30V, 2A) is used to enable the user to choose the required voltage; the voltage across the standard reference resistance was measured by digital multimeter. The thick film samples were heated slowly to avoid any thermal runway. At the selected interval of temperature voltage across the reference resistance was noted. The resistance of thick film sample was calculated by using the Equation 1.

$$R_{sample}=R_{ref}\,[V_{supply}/V_{ref}] \quad \text{.....(1)}$$

Where, R_{sample} –Resistance of thick film,
R_{ref} – Resistance of Standard reference resistance,
V_{supply} – Applied voltage,
V_{ref} –Reference voltage across standard resistance.

Fig.1. Schematic diagram for static measurement system

2) Structural and Morphological Studies

Using X-ray diffraction (Miniflex Model, Rigaku, Japan) analysis from 20-80, 2θ was carried out to examine the phases of the SnO_2 films samples. The instrumental broadening was removed using silicon standard sample. The single line approximation method has adopted for the crystallite size determination using most intense peak. The average grain size of tin oxide thick film sample was calculated by using the Scherer formula [14]:

$$D=\frac{0.9\lambda}{\beta COS\theta} \quad \text{.....(2)}$$

Where, D- is the average grain size,
λ-1.542 Å (X-ray wavelength),
β - the peak FWHM in radiation,
θ-diffraction peak position.

The microstructure and chemical composition of the films were analyzed using a scanning electron microscope [Nova nano SEM NPEP303] coupled with an energy dispersive spectrometer (EDS JEOL, JED-2300, Germany). In FTIR analysis, the IR spectra have been recorded in the range of frequencies 500-5000 cm^{-1}. FTIR spectra were recorded using PERKIN ELMER instrument using KBr pellets (1% Wt/Wt) with spectal resolution of 2 cm^{-1} and taking 32 scans for each sample. UV analysis was performed in SHIMADZU UV-2600 UV-VIS Spectrophotometer with wide range of 200-800 nm with single scan mode and fast scan speed.

IV. RESULTS AND DISCUSSIONS

A. Structural Characteristics

1) X-ray Diffraction Analysis: In Order to understand the crystalline phases in SnO_2 thick film samples, the X-ray diffraction study was undertaken. XRD analysis was performed using CuKα radiation of wavelength λ=1.54Å at accelerating voltage of 40 kV and 40 mA current in continuous scan mode with 15 degree/min used for phase and crystal structure study of the deposited thick films at room temperature. Fig. 2 shows an XRD pattern of SnO_2 film samples plotted in the range 20-80 (2θ) verses intensity having several peaks of tin oxide phases showing polycrystalline nature. Peaks are observed at the angular positions: 2θ= 26.94, 34.26, 38.34, 38.48, 52.1, 55.1, 62.22, 65.04 and 66.22 which were indexed to the (110), (101), (200), (111), (211), (220), (310), (112) and (301) respectively. The observed peaks match well with the reported data of Tin-oxide (JCPDS Card No. 41-1445) confirming the polycrystalline nature. The higher peak intensities in XRD pattern at 2θ=26.94 is due to the better crystalinity and bigger grain size can be attributed to the agglomeration of particles. The narrow and sharp peaks reveal that SnO_2 compositions are well crystallized. The crystallite size of highly crystalline peak indexed at (110) is found to be 115.04 nm. The average crystallite size was calculated Using Scherer equation and was estimated to be about 93.34 nm.

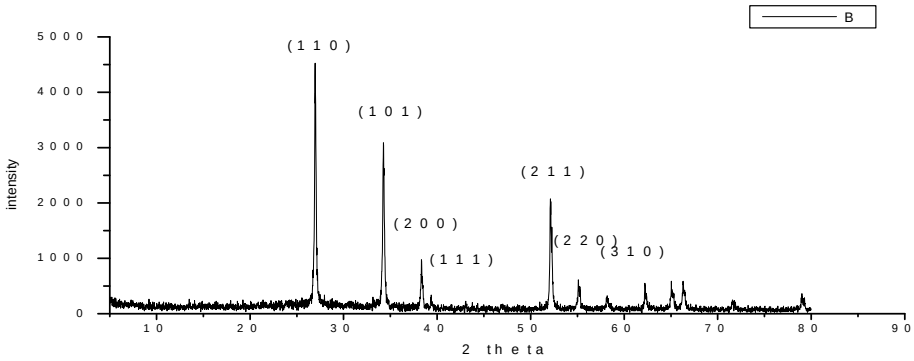

Fig.2. XRD pattern of SnO_2 film sample fired at 450^0C

Table 1. Indicates XRD parameters

2θ	FWHM	planes	Crystallite size in nm
26.94	0.071	110	115.04
34.26	0.165	101	50.37
38.34	0.094	200	89.46
38.48	0.071	111	118.49

2) *Scanning Electron Microscopy:* Scanning electron microscopy is sophisticated technique to study the microstructure of thick film samples. Fig. 3 shows the surface morphology of SnO_2 films observed by SEM. SEM image is recorded at 200000x magnification range with 15 kV accelerating voltage for SnO_2 thick film sample fired at 450^0C. The micrograph of this sample shows voids between the particles, basically due to evaporation of the organic solvent during the firing of the film. The average calculated particle diameter in this micrograph is around 45.53 nm. More agglomeration in the film samples are observed in tin oxide micrograph which will be better for gas sensing study in future.

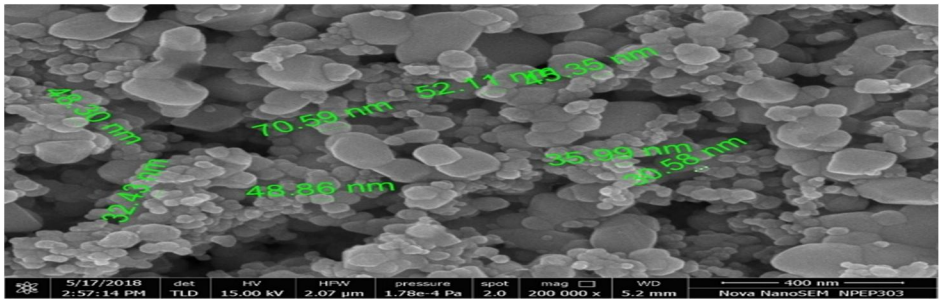

Fig 3. SEM image of SnO_2 thick film

3) *Energy Dispersive X-Ray Analysis:* The EDX analysis always used to examine the composition of the film materials through qualitative and quantitative approach with 1000 ppm detection limit or 0.1% wt. The thick film SnO_2 was coated with sputtered platinum with 2-3 nm. Fig.3 illustrates the composition of SnO_2 thick film. It is seen that the major peaks observed are of tin and oxygen and no other impurity present in the tin oxide composition. Also the spectra reveals that weight % and atomic % are nearly matched as illustrated in table no .2.

Table-2: Quantitative elemental analysis

Element	Series	Wt. %	At. %
Sn	L-series	72.33	26.05
O	K-series	27.67	73.95
	Total	100.00	100.00

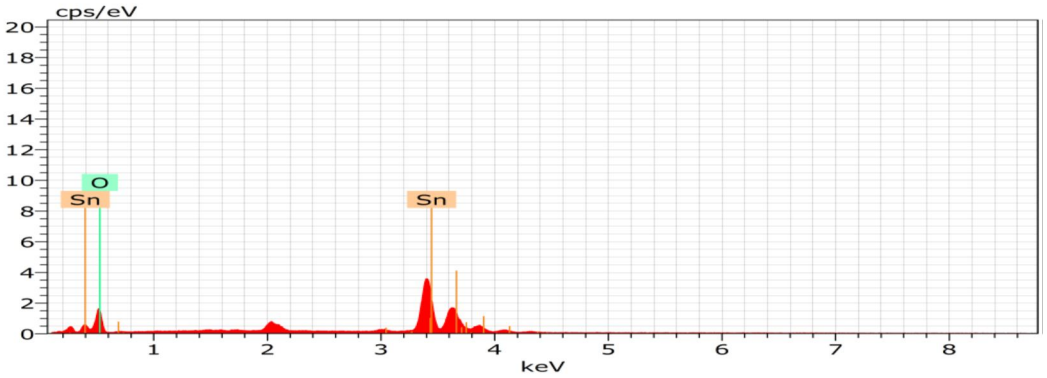

Fig. 4. EDAX curve of SnO_2

4) *Ftir Analysis:* The absorption band at 3734 cm^{-1} is due to attribution of asymmetric hydroxyl stretching mode of (O-H non bonded) vibration of surface hydroxyl group or adsorbed water[15]. IR band at 2949 cm^{-1} is due to C-H bond is observed. An important characteristic peak is observed at 1514 cm^{-1} an overtone of asymmetric stretching mode of surface bridging oxide formed by condensation of adjacent surface hydroxyl groups Sn-O-Sn atomic linkages. 675 cm^{-1} is due to stretching frequency O-Sn-O atoms where vibrations and lattice modes were observed[16].

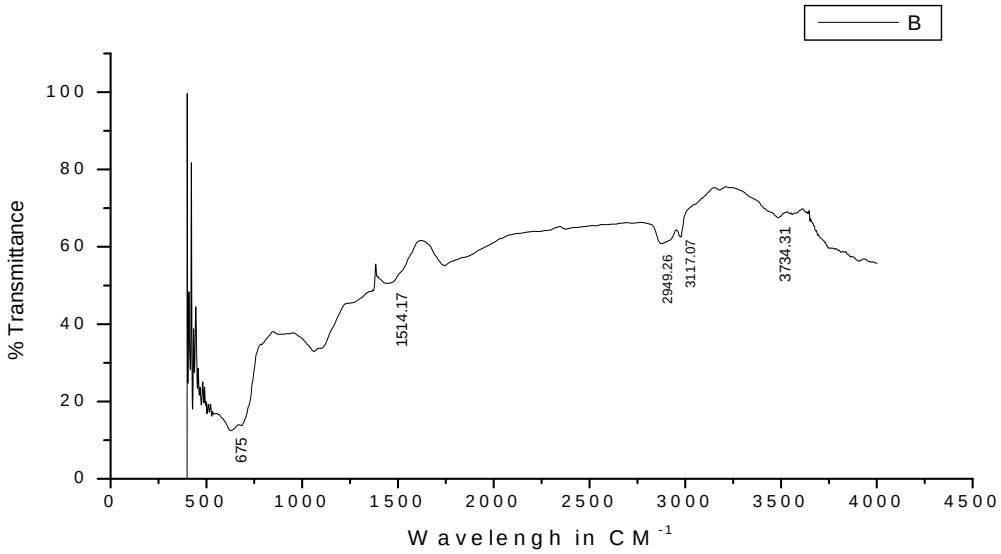

Fig 5. FTIR spectra of SnO_2

5) *UV Analysis:* Optical absorption spectroscopy is most traditional method by which quantum effects in semiconducting nanomaterial can be studied. Optical absorption analysis has been extensively proven to be a vital and active tool in interpreting the increase or decrease of energy gap and thereby progress of discrete characteristic in the spectra can be revealed. Thus study of optical properties of material is important due to capability of technique to give information in the electronic band, structures, localized states, Trapping levels and electronic transitions. For absorption study, a sample of 10 mg SnO_2 powder is dissolved in 10 ml water solution (1N H_2SO_4 solvent) to prepare 1000 ppm or 10 µg/ml concentration. The band gap of SnO_2 was calculated following tauc's equation 3,

$$(\alpha h\upsilon)^{1/n}=A(h\upsilon-E_g) \quad \text{.....(3)}$$

Where E_g is the band gap, A is energy independent constant, n=1/2 for direct band gap of material, α is absorption coefficient, hυ is incident photon energy where h is Planck's constant and υ is frequency. The extrapolated linear portion to horizontal axis of the tauc's plot gives value of band gap. The calculated band gap value is 3.18 eV which attributes to red shift. The absorption edge in SnO_2 material arises due to larger grain size, thermal effects and reduction in thickness of the film[17].

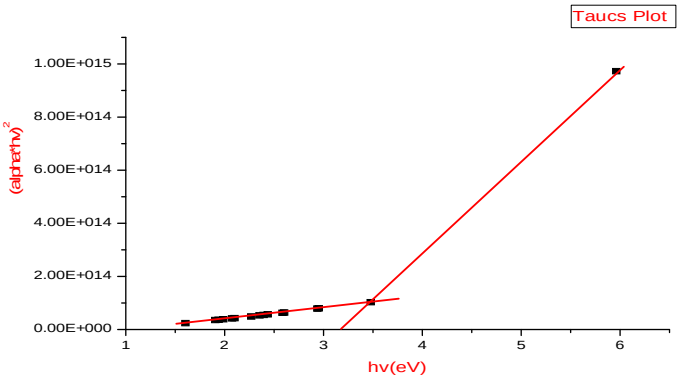

Fig 6. UV spectra of SnO_2

B. Resistance Measurement

1) NTC Characteristics: Fig. 7 shows the resistance variation of the SnO_2 thick film as a function of temperature. In the low temperature range (room temperature to around 280 °C), a decrease in resistance was observed as increasing the temperature due to the release of the carriers [16]. The tin oxide nanoparticles were having the conductivity even at low temperature also due to the migration of charged species like O^{2-}, O^-, OH^- and H_3O^+ [18].

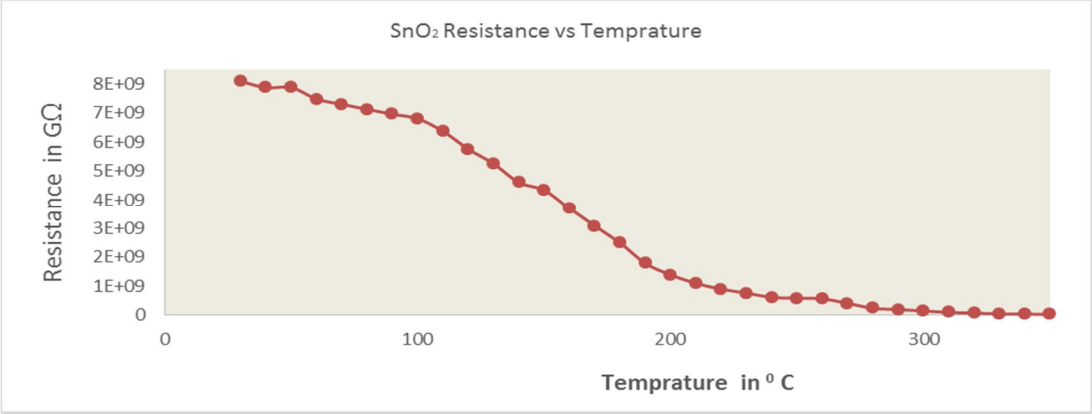

Fig 7. Indicates the NTC Charectristics of SnO_2 Base material

2) Activation Energy graph: The activation energy of the electron transport in coduction band is determined from arrhenius plot log R vereses 1/T. following graph indicates that curve has two distinct regions of low and high temprature region.

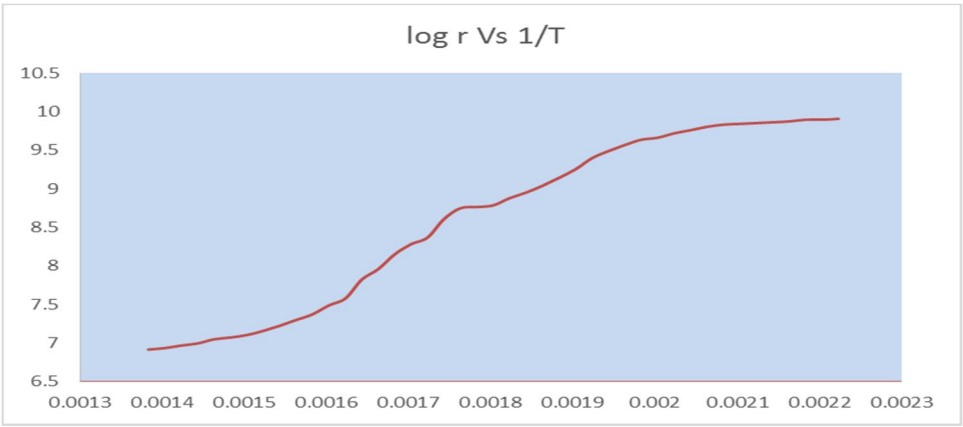

Fig 8. Indicates the arrhenius plot of SnO_2 Base material

V. CONCLUSION

The thick film of SnO_2 prepared by screen printed method fired at high temperature (450^0C) give rise to new characteristic properties in nanomaterial rather than bulk one or macro level. The XRD data shows high degree of polycrystalline nature with average crystallite size 93.34 nm. SEM micrograph depicts particle size about 45.52 nm. The elemental data is well concurrent with standard composition of SnO_2 in terms of atomic and weight percentage. The IR spectra have been recorded in the range of frequencies 500-5000 cm^{-1} which shows many broad bands between 2800-4000 cm^{-1}. Electrical characterization clearly indicates that at low temperature film resistance is high attributed to the thick films of SnO_2 prepared by standard screen printing method exhibit negative temperature coefficient. Ultraviolet absorption spectrum of pure SnO_2 shows that SnO_2 particles are monodispersed and shows broad absorption peak at 3.18 eV.

REFERENCES

[1] L. I. Nadaf, K. S. Vankatesh Synthesis and characterization of Tin oxide nanoparticles by co-precipitation method, IOSR-Journal of applied chemistry 9, 2016 PP 01-04
[2] S. Kannan,N. P. Subiramaniyam, M. Satishkemar, Synthesis and Characterization of tin oxide: A Review, Int. Jou. For res. In applied sci.&engee. Tech, Volume 5, issue XI. 2017 ISSN:2321-9653
[3] T.Krishnakumar, R. Jayaprakash, V.N. Singh, and B.R. Mehta, A. R. Phani, Synthesis and characterization of tin oxide nanoparticle for humidity sensor applications, Journal of Nano Research Vol. 4 (2008) pp 91-101
[4] Michael A. Tarshelli, In Your Element, Springer Nature, Nature chemistry Vol 9, 2017, pp 500
[5] Hyoun Woo Kim,, Nam Ho Kim, Ju Hyun Myung, and Seung Hyun Shim, Characteristics of SnO2 fishbone-like nanostructures prepared by the thermal evaporation phys. stat. sol. (a) 202, No. 9, 1758–1762 (2005),
[6] Matthias Batzill, Surface Science Studies of Gas Sensing Materials: SnO2 Sensors 2006, 6, 1345-1366
[7] S. G. Ansari, P. Boroojerdian, S. K. Kulkarni, S. R Sainkar, R. N. Karekar, R. C. Aiyer, Effect of Thickness on H2gas sensitivity of SnO2 nano particles based thick film resistors, Journal of Materials Science: Materials in Electronics, 7, 1996, pp. 267-270.
[8] Maria Prudenziati; Bruno Morten, Thick film Sensors. An Overview, Sensors and Actuators, 10, 1986, pp. 65-82.
[9] Harper C. A, Handbook of Thick film hybrid Microelectronics, McGraw Hill Book Co., New York, 1974.
[10] Kiran Jain, R. B Pant, S. T. Laxmikumar, Effect of Ni doping on thick film SnO2gas Sensor, Sensors and Actuators, B, 113, 2006, pp. 823-829.
[11] Ramkumar K., Thick Film Deposition and Processing, short term course on thin and thick Film hybrid Microelectronics, Bangalore, 1986.
[12] A. T. Nimal, Vijay Kumar and A. K. Gupta, Superconducting transition edge bolometer based on single phase BPSCCO2223 thick film, Indian Journal of pure and applied physics, Vol. 42, 2004, pp. 275-278.
[13] L. A. Patil, Wani P. A., Sainkar S. R., Mitra A., Pathak G. J. and Amalnerakar D. P., Studies on “fritted” thick films of photoconducting CdS, Mater. Chem. Phys, 55, 1998, p.79
[14] K. Chatterjee, S. Chatterjee, A. Banerjee, M. Raut, NC. Pal, A. Sen, HS. Maiti, The effect of palladium incorporation on methane sensitivity of antimony doped tin dioxide, Mater. Chem. and Phys. 81 (2003) 33-38.
[15] B. D. Cullity, Elements of X-ray diffraction, Addison-Wesley Publishing Co. 1956.
[16] Jianrong Zhang, Lian Gao, Synthesis and characterization of antimony doped Tin oxide (ATO) nanoparticle, Inorg. Chem. Commun. 7 (2004) 91-93.
[17] Saloni Goyal, Chauhan R. P., Effect of Ar+ ion implantation on the properties of electrodeposited CdTe thin films Bulletin of material sciences, 41:131 2018 doi 10.1007/s12034-018-1649-4
[18] U. Weimer, W. Gopal, A.C measurements on tin oxide sensors to improve selectivities and sensitivities, Sens. Actuators B 26 (1995) 13-18.

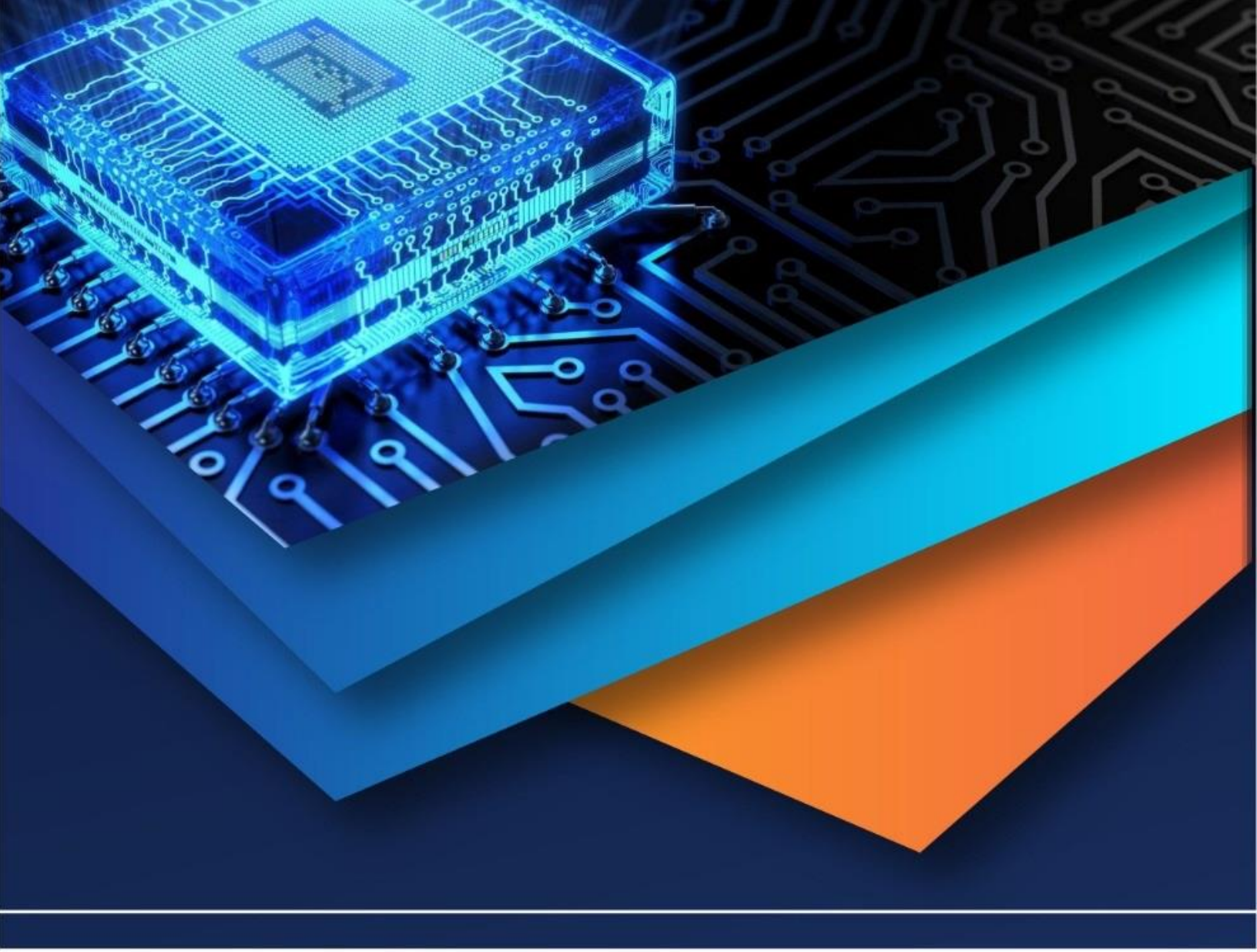

10.22214/IJRASET

45.98

IMPACT FACTOR: 7.129

IMPACT FACTOR: 7.429

INTERNATIONAL JOURNAL FOR RESEARCH

IN APPLIED SCIENCE & ENGINEERING TECHNOLOGY